SUSY DARK MATTER

S. KRAML
LPSC, 53 av des Martyrs, 38026 Grenoble, France
email: sabine.kraml@lpsc.in2p3.fr

Collider searches for new physics and direct searches for dark matter are important topics at this conference. In this contribution, I discuss their potential synergy and complementarity by means of the minimal supersymmetric standard model with a neutralino dark matter candidate.

1 Introduction

Cosmological data ranging from the cosmic microwave background to rotation curves of spiral galaxies tell us that most of the mass in the Universe is provided by non-luminous, hence 'dark' matter [1,2,3]. More precisely, the recent measurements from WMAP [4] and SDSS [5] imply a (dominantly cold) dark matter density of $\Omega h^2 \simeq 0.1$ to an accuracy of about 10%.[a] The nature of this dark matter is one of the big open questions of present-day physics. Many lines of reasoning suggest, however, that it consists of a new weakly interacting massive particle, a so-called WIMP.

At the same time, we know that the Standard Model (SM) of particle physics, despite its tremendous success at energies up to ~ 100 GeV, is incomplete. In attempts to embed the SM in a more fundamental frame, theorists have come up with a wealth of Beyond the Standard Model (BSM) theories, which typically predict new particles and phenomena at the TeV energy scale. To probe this exciting new frontier is indeed the primary motivation to build the LHC! It is even more exciting that the lightest of these new BSM particles is often stable by virtue of a new discrete symmetry (introduced to match electroweak precision measurements and/or the non-observation of proton decay) and hence provides a natural dark matter candidate.

The dark matter candidates such put forth by particle physics are quite numerous [3] and contain, for example, the lightest supersymmetric particle in supersymmetry with R-parity con-

[a] The exact mean value and error depend on the data combination and number of parameters fitted, see Ref. [6].

Standard Model particles and fields		Supersymmetric partners			
		Interaction eigenstates		Mass eigenstates	
Symbol	Name	Symbol	Name	Symbol	Name
$q = d, c, b, u, s, t$	quark	$\tilde{q}_L$, $\tilde{q}_R$	squark	$\tilde{q}_1$, $\tilde{q}_2$	squark
$l = e, \mu, \tau$	lepton	$\tilde{l}_L$, $\tilde{l}_R$	slepton	$\tilde{l}_1$, $\tilde{l}_2$	slepton
$\nu = \nu_e, \nu_\mu, \nu_\tau$	neutrino	$\tilde{\nu}$	sneutrino	$\tilde{\nu}$	sneutrino
g	gluon	$\tilde{g}$	gluino	$\tilde{g}$	gluino
$W^\pm$	W-boson	$\tilde{W}^\pm$	wino		
H^-	Higgs boson	$\tilde{H}_1^-$	higgsino	$\tilde{\chi}^\pm_{1,2}$	chargino
H^+	Higgs boson	$\tilde{H}_2^+$	higgsino		
B	B-field	$\tilde{B}$	bino		
W^3	W^3-field	$\tilde{W}^3$	wino		
H_1^0	Higgs boson			$\tilde{\chi}^0_{1,2,3,4}$	neutralino
H_2^0	Higgs boson	$\tilde{H}_1^0$	higgsino		
H_3^0	Higgs boson	$\tilde{H}_2^0$	higgsino		

Table 1: Standard Model particles and their superpartners in the MSSM [3].

servation; the lightest Kaluza–Klein (KK) excitation in models with extra dimensions and KK-parity; the lightest T-odd state in little Higgs models with T-parity; etc. Note that all these possibilities are generally testable in collider experiments. This creates a strong interplay [7,8] between particle physics, astrophysics and cosmology, at both theoretical and experimental levels.

2 Supersymmetry

Of the existing BSM theories, supersymmetry (SUSY) [9] is arguably the best motivated one. SUSY is a symmetry between fermions and bosons. A SUSY generator Q changes a fermion into a boson and vice versa:

$$Q|\text{fermion}\rangle = |\text{boson}\rangle\,, \quad Q|\text{boson}\rangle = |\text{fermion}\rangle\,. \tag{1}$$

This is an extension of space-time to include anti-commuting coordinates $x^\mu \to (x^\mu, \theta^\alpha)$ with $\{\theta^\alpha, \theta^\beta\} = \varepsilon^{\alpha\beta}$, combining the relativistic 'external' symmetries (such as Lorentz invariance) with the 'internal' symmetries of a field, such as weak isospin. It is in fact the unique(!) extension of the Poincaré algebra (the algebra of space-time translations, rotations and boosts).

From the phenomenological point of view, SUSY predicts a partner particle, a so-called 'superpartner' or 'sparticle', for every SM state.[b] The particle content of the Minimal Supersymmetric Standard Model (MSSM), is given in Table 2. In its local gauge theory version, SUSY also includes spin-2 and spin-3/2 states, the graviton and its superpartner the gravitino and is hence potentially capable of connecting gravity with the other interactions (so-called supergravity or short SUGRA). A few more things are important to observe:

i) SUSY must be a broken symmetry, else SM particles and their superpartners would have equal mass. In order to still solve the hierarchy problem of the SM (i.e. to stabilize the electroweak scale against quadratically divergent radiative corrections) and to achieve gauge-coupling unification, one expects the superpartners to have masses of $m \leq \mathcal{O}(1)$ TeV.

ii) After electroweak symmetry breaking, we are left with three neutral Higgs bosons: two scalars h, H and one pseudoscalar A. Moreover, sparticles with the same SU(3)×U(1) quantum numbers mix, c.f. Table 2. In particular, the bino, wino and neutral higgsinos mix to mass eigenstates called neutralinos $\tilde{\chi}^0_{1,\ldots,4}$ (with $\tilde{\chi}^0_1$ the lightest one by definition).

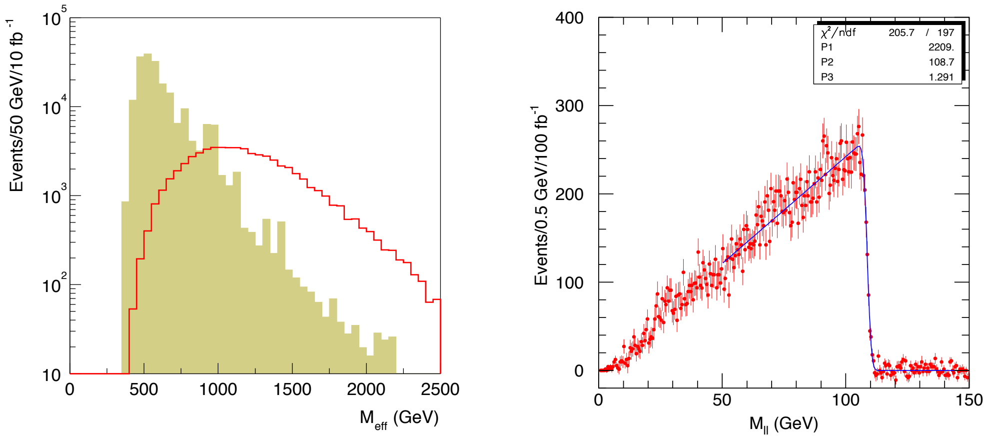

Figure 1: Left: $M_{\rm eff}$ distribution for a SUGRA point with gluino and squark masses of about 700 GeV (histogram) and Standard Model background (shaded) after cuts. Right: Di-lepton invariant-mass distribution from $\tilde\chi^0_2 \to \tilde l^\pm l^\mp \to l^+l^-\tilde\chi^0_1$ decays. From [15].

iii) If SUSY comes with a new conserved parity, so-called R-parity, under which SM particles are even and SUSY particles are odd, the lightest supersymmetric particle (LSP) is stable. in this case it has to be electrically and colour neutral and constitutes a natural dark matter candidate.

In the following I concentrate on the MSSM with a neutralino LSP. For gravitino dark matter, which has a quite different phenomenology, I refer to the contribution by F. Steffen in these proceedings. Sneutrinos in extensions of the MSSM are discussed by C. Arina in the YSF.

3 Collider searches

If low-scale supersymmetry is realized in Nature, experiments at the LHC have excellent prospects to discover it [10,11,12]. In particular, squarks and gluinos should be copiously produced at the LHC through the QCD interaction, with cross sections of $\mathcal{O}(1)$ pb for masses around 1 TeV.

This is followed by (multi-step) decays into lighter sparticles. Squarks decay into gluinos plus jets, $\tilde q \to q\tilde g$, if kinematically allowed, or into charginos/neutralinos plus jets, $\tilde q_L \to q'\tilde\chi^\pm_i,\, q\tilde\chi^0_j$ and $\tilde q_R \to q\tilde\chi^0_j$ $(i=1,2;\; j=1,...,4)$. Gluinos always decay into squarks, either in the two-body mode $\tilde g \to q\tilde q$ if kinematically open, or else $\tilde g \to q\bar q'\tilde\chi^\pm_i,\, q\bar q\tilde\chi^0_j$ via an off-shell squark. The charginos $\tilde\chi^\pm_{1,2}$ and neutralinos $\tilde\chi^0_{2,3,4}$ decay further, e.g. $\tilde\chi^\pm_i \to W^\pm\tilde\chi^0_j$ or $\tilde\chi^0_k \to Z\tilde\chi^0_j$, until the LSP $\tilde\chi^0_1$ is reached. The LSP, being stable and neutral, escapes undetected.

SUSY events are hence characterized by multiple hard jets, maybe accompanied by leptons, plus large missing transverse energy $E_T^{\rm miss}$. The significance of such a signal over the SM background is illustrated in the left plot in Fig. 1, which shows the number of events as a function of the 'effective mass' computed from the missing energy and the momenta of the hardest jets, $M_{\rm eff} = E_T^{\rm miss} + \sum p_T^{\rm jets}$. Note that the y-axis is log-scale! The $M_{\rm eff}$ distribution also provides a first estimate of the gluino/squark mass scale.

In certain scenarios and/or with high enough statistics, electroweak production of charginos and neutralinos, e.g., $pp \to \tilde\chi^\pm_1\tilde\chi^\mp_1,\, \tilde\chi^\pm_1\tilde\chi^0_2$, can also be important. The latter process can lead to the goldplated tri-lepton signal, which is also searched for at the Tevatron [13]. Moreover, for slepton masses up to 300 GeV, slepton-pair production can lead to detectable di-lepton signals.

The discovery of SUSY particles will be followed by detailed measurements of their masses and decay properties. Since the LSP escapes as missing energy, no mass peaks can be reconstructed. Instead, mass measurements exploit kinematic distributions in cascade decays [14,15]. For

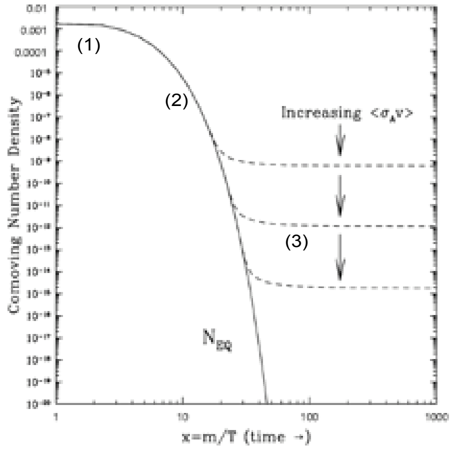

Figure 2: The cosmological evolution of a thermal relic's comoving number density, from [1]. The full line is the equilibrium abundance; the dashed lines are the actual abundance after freeze-out. As the annihilation cross section $\langle\sigma_A v\rangle$ is increased, the WIMP stays in equilibrium longer, leading to a smaller relic density.

instance, the invariant-mass distribution of the leptons stemming from the chain $\tilde\chi^0_2 \to l^\pm \tilde l^\mp \to l^+l^-\tilde\chi^0_1$ has a triangular shape with a sharp endpoint at $M_{ll}^{\rm max} = [(m^2_{\tilde\chi^0_2} - m^2_{\tilde l})(m^2_{\tilde l} - m^2_{\tilde\chi^0_1})/m^2_{\tilde l}\,]^{1/2}$, which can be measured very precisely, see the right plot in Fig. 1. If the leptons come from the three-body decay $\tilde\chi^0_2 \to l^+l^-\tilde\chi^0_1$, M_{ll} has a different shape and an endpoint at $m_{\tilde\chi^0_2} - m_{\tilde\chi^0_1}$. Additional distributions can be constructed involving jets stemming from gluino and squark decays. This way the masses of the sparticles appearing in the decay chains can be reconstructed.

Let us finally come back to the dark matter question. The alert reader will have noticed that because of R-parity sparticles are produced in even numbers, and every sparticle decay terminates in the LSP. As a consequence, each SUSY event contains two LSPs. Moreover, if squarks and gluinos weigh about 1 TeV, we expect of the order of 100 events/day —at low luminosity. The LHC may hence well turn out as a dark matter factory, where the nature and properties of dark matter candidates may be studied in a controlled environment.

Typical precisions at the LHC are $\mathcal{O}(10\%)$. Much higher precisions at the percent to permil level might be achieved at an International e^+e^- Linear Collider (ILC) [16]. The determination of neutralino dark matter properties at LHC and ILC has been analyzed, e.g., in [17].

4 Relic density

The standard cosmological scenario assumes that the dark matter particle, let us call it χ, is a thermal relic of the Big Bang as illustrated in Fig. 2: When the early Universe was dense and hot, $T \gg m_\chi$, χ was in thermal equilibrium; annihilation of χ and $\bar\chi$ into lighter particles, $\chi\bar\chi \to l\bar l$, and the inverse process $l\bar l \to \chi\bar\chi$ proceeded with equal rates. As the Universe expanded and cooled to a temperature $T < m_\chi$, the number density of χ dropped exponentially, $n_\chi \sim e^{-m_\chi/T}$. Eventually the temperature became too low for the annihilation to keep up with the expansion rate and χ 'froze out' with the cosmological abundance observed today.

The time evolution of the number density $n_\chi(t)$ is described by the Boltzman equation,

$$ {\rm d}n_\chi/{\rm d}t + 3Hn_\chi = -\langle\sigma_A v\rangle\,[(n_\chi)^2 - (n_\chi^{\rm eq})^2]\,, \tag{2}$$

where H is the Hubble expansion rate, $n_\chi^{\rm eq}$ is the equilibrium number density, and $\langle\sigma_A v\rangle$ is the thermally averaged cross section times the relative velocity of the annihilating particles. The relic density today turns out to be inversely proportional to the annihilation cross section,

$\Omega_\chi h^2 \propto 1/\langle\sigma_A v\rangle$. Note that $\langle\sigma_A v\rangle$ includes a sum over all possible annihilation channels for the LSP. These are annihilation into gauge boson pairs through t-channel chargino and neutralino exchange, and annihilation into fermion pairs through t-channel sfermion exchange and s-channel Z/Higgs exchange. Moreover, co-annihilation channels involving sparticles that are close in mass to the LSP have to be taken into account. For details of the calculation, see [2,18].

The relic density of the LSP hence depends on all the MSSM masses and couplings that enter the different annihilation/co-annihilation channels. On the one hand, this is often used to severely constrain SUSY models by demanding that the relic density of the LSP falls within the WMAP–SDSS range (see the YSF contribution by S. Sekmen for an example). On the other hand, if the masses and couplings of SUSY particles are measured precisely enough, $\Omega_\chi h^2$ can be computed and compared to the cosmologically observed value.

Here notice that the standard picture heavily relies on two assumptions: i) that the initial temperature after inflation has been high enough to fully thermalize the LSP and ii) that the entropy per comoving volume has been constant below the freeze-out temperature. In non-standard scenarios with low reheat temperature and/or late entropy production, the relic density can be quite different from the value in the standard scenario. A precise determination of the LSP annihilation cross section from collider experiments, together with a confirmation that the LSP is indeed the cold dark matter through direct detection (see next section), will hence allow to probe these asumptions [19], i.e. probe the evolution of the early universe up to the freeze-out temperature $T_f \sim m_\chi/20$.

5 Direct detection

Experiments such as CDMS [20], XENON [21], ZEPLIN [22], EDELWEISS [23], CRESST [24], KIMS [25] and COUPP [26] aim at detecting WIMPs through their elastic scattering with nuclei. The current experimental limits and projected sensitivities are shown in Fig. 3, together with predictions from various MSSM scenarios. Principally one distinguishes two classes, spin-dependent and spin-independent interactions. On the partonic level, WIMP interactions with quarks and gluons in the nucleons contribute.

In the case of neutralino dark matter, the scattering off quarks can occur through t-channel exchange of Z or CP-even Higgs bosons, or s-channel exchange of squarks:

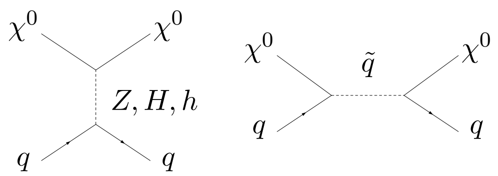

The diagrams with Z and squark exchange contribute to the axial-vector (spin) interaction, $\mathcal{L} \sim \bar\chi\gamma^\mu\gamma^5\chi\bar q\gamma_\mu\gamma_5 q$. The Higgs and squark exchange diagrams contribute to the scalar (spin-independent) interaction, $\mathcal{L} \sim \bar\chi\chi\bar q q$. The neutralino interaction with gluons proceeds through quark and squark loops and contributes to the spin-independent cross section. See [2,27] for details. Note that since the neutralino is a Majorana particle, there is no vector interaction of the form $\mathcal{L} \sim \bar\chi\gamma^\mu\chi\bar q\gamma_\mu q$.

The effective neutralino–nucleon coupling hence depends on the neutralino mass and decomposition (i.e. the bino/wino/higgsino content) as well as on the Higgs and squark masses and couplings. Again, if the supersymmetric spectrum is known from collider experiments, the scattering cross section can be predicted.[c] A word of caution is, however, in order here because the strange content of the nucleon is not known well; this induces a considerable uncertainty [29] in the neutralino–nucleon cross section, in particular if Higgs exchange dominates. Finally, the

[c] This cross section also determines the rate at which neutralinos would accrete in the Earth and Sun.

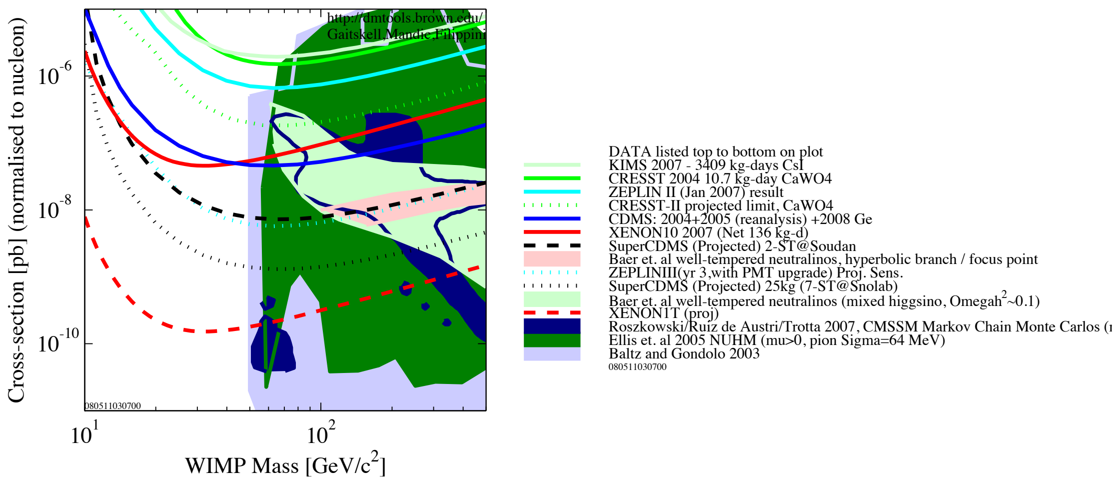

Figure 3: Direct detection of WIMP dark matter: current experimental limits and projected sensitivities, together with various SUSY model predictions; generated with `DMTOOLS` [28].

neutralino–nucleon cross sections $\sigma_{\chi n}$ and $\sigma_{\chi p}$ have to be translated to the neutralino–nucleus scattering cross section $\sigma_{\chi N}$ applying nuclear form factors.

The actual direct-detection rate depends, moreover, on the local dark matter density ρ_χ and the velocity distribution $f(v)$. Roughly speaking, the rate of events per day and per kg of detector material is $R \sim \rho_\chi \sigma_{\chi N} \langle v \rangle / (m_\chi m_N)$, with m_N the target nucleus mass and $\langle v \rangle$ the average velocity of χ relative to the target. Typical estimates are $\rho_\chi = 0.22 - 0.73$ GeV/cm^3 and $\langle v \rangle = 230 \pm 20$ km/s. If m_χ and $\sigma_{\chi N}$ are known with good precision, the local density and velocity distribution can be tested.

At this point, let me stress the importance of direct detection for another reason: Although collider experiments may identify a dark matter candidate and precisely measure its properties, they will not be able to distinguish a cosmologically stable from a very long-lived but unstable particle. Therefore validation of the collider signal through direct detection is essential. The key to this is the WIMP mass, which may be determined [30,31] in direct-detection experiments through the distribution of the recoil energy, $E_R \propto 2v^2 m_N/(1 + m_N/m_\chi)^2$. Note that E_R is sensitive to small m_χ but becomes almost constant for $m_\chi \gg m_N$. Note also the velocity dependence, which is source of considerable uncertainty in a single experiment. This may be evaded by using multiple targets [31]. Precisions are, however, still poor for $m_\chi \gg m_N$.

6 Conclusions

For conclusions, let me cite G. F. Giudice in "Theories for the Fermi scale" [32]: *It is impossible to overestimate the importance of discovering dark matter at the LHC. Such a discovery will imply a revision of the SM, it will strenghten the connection between particle physics, cosmology and astrophysics, and it will enormously enlarge our understanding of the present and past universe.*

So be prepared for exciting times at future Moriond meetings.

Acknowledgments

I wish to thank the organisers for creating a remarkably pleasant and inspiring atmosphere. Fruitful discussions with other participants are also gratefully acknowledged.

References

1. E. W. Kolb and M. S. Turner, *The Early universe*, Front. Phys. **69** (1990) 1.
2. G. Jungman, M. Kamionkowski and K. Griest, Phys. Rept. **267** (1996) 195, hep-ph/9506380.
3. G. Bertone, D. Hooper and J. Silk, Phys. Rept. **405** (2005) 279, hep-ph/0404175.
4. D. N. Spergel *et al.*, Astrophys. J. Suppl. **170** (2007) 377, astro-ph/0603449; E. Komatsu *et al.*, arXiv:0803.0547 [astro-ph].
5. M. Tegmark *et al.*, Phys. Rev. **D69** (2004) 103501, astro-ph/0310723.
6. J. Hamann, S. Hannestad, M. S. Sloth and Y. Y. Y. Wong, Phys. Rev. D **75** (2007) 023522, astro-ph/0611582.
7. D. Hooper and E. A. Baltz, arXiv:0802.0702 [hep-ph].
8. H. Baer and X. Tata, arXiv:0805.1905 [hep-ph].
9. See e.g., H. Baer and X. Tata, *Weak scale supersymmetry: From superfields to scattering events*, Cambridge University Press (2006).
10. ATLAS Collaboration, *ATLAS Detector and Physics Performance: Technical Design Report*, vol. 2, ATLAS-TDR-15, CERN-LHCC-99-15 (1999).
11. CMS Collaboration, *CMS Physics: Technical Design Report, Volume 2: Physics Performance*, CMS-TDR-8.2, CERN-LHCC-2006-021 (2006).
12. S. Tsuno, these proceedings.
13. S. Dube, these proceedings.
14. I. Hinchliffe, F. E. Paige, M. D. Shapiro, J. Soderqvist and W. Yao, Phys. Rev. D **55** (1997) 5520, hep-ph/9610544.
15. H. Bachacou, I. Hinchliffe and F. E. Paige, Phys. Rev. D **62** (2000) 015009, hep-ph/9907518.
16. G. Weiglein *et al.*, Phys. Rept. **426** (2006) 47, hep-ph/0410364; `http://www.linearcollider.org`.
17. E. A. Baltz, M. Battaglia, M. E. Peskin and T. Wizansky, Phys. Rev. D **74** (2006) 103521, hep-ph/0602187.
18. M. Drees and M. M. Nojiri, Phys. Rev. D **47** (1993) 376, hep-ph/9207234.
19. M. Drees, H. Iminniyaz and M. Kakizaki, Phys. Rev. D **76** (2007) 103524, arXiv:0704.1590 [hep-ph], and references therein.
20. Z. Ahmed *et al.*, arXiv:0802.3530 [astro-ph]; D. S. Akerib *et al.*, Phys. Rev. D **73** (2006) 011102, astro-ph/0509269.
21. J. Angle *et al.*, Phys. Rev. Lett. **100** (2008) 021303, arXiv:0706.0039 [astro-ph]; R. Santorelli, these proceedings.
22. G. J. Alner *et al.*, Astropart. Phys. **28** (2007) 287, astro-ph/0701858.
23. V. Sanglard *et al.*, Phys. Rev. D **71** (2005) 122002, astro-ph/0503265.
24. G. Angloher *et al.*, Astropart. Phys. **23** (2005) 325 , astro-ph/0408006; R. F. Lang, these proceedings.
25. H. S. Lee. *et al.*, Phys. Rev. Lett. **99** (2007) 091301, arXiv:0704.0423 [astro-ph]; S. K. Kim, these proceedings.
26. W. J. Bolte *et al.*, J. Phys. Conf. Ser. **39** (2006) 126; M. Szydagis, these proceedings.
27. M. Drees and M. Nojiri, Phys. Rev. D **48** (1993) 3483 [arXiv:hep-ph/9307208].
28. R. Gaitskell, V. Mandic and J. Filippini, `http://dmtools.berkeley.edu/limitplots/`
29. J. Ellis, K. A. Olive and C. Savage, Phys. Rev. D **77** (2008) 065026, arXiv:0801.3656 [hep-ph]; G. Belanger, F. Boudjema, A. Pukhov and A. Semenov, arXiv:0803.2360 [hep-ph].
30. A. M. Green, JCAP **0708** (2007) 022, hep-ph/0703217; arXiv:0805.1704 [hep-ph].
31. M. Drees and C. L. Shan, arXiv:0803.4477 [hep-ph].
32. G. F. Giudice, arXiv:0710.3294 [hep-ph].